Geminal Dimethyl Substitution Enabled Controlled Ring-Opening Polymerization and Selective Depolymerization of Penicillamine-Derived β-Thiolactones

Wei Xiong,[a] Wenying Chang,[a] Dong Shi,[a] Lijiang Yang,[b] Ziyou Tian, [a] Hao Wang, [a] Zhengchu Zhang,[a] Xuhao Zhou,[a] Erqiang Chen,[a,*] and Hua Lu[a,*]

[a] Beijing National Laboratory for Molecular Sciences, Center for Soft Matter Science and Engineering, Key Laboratory of Polymer Chemistry and Physics of Ministry of Education, College of Chemistry and Molecular Engineering, Peking University, Beijing 100871, People's Republic of China;

[b] Institute of Theoretical and Computational Chemistry, Biodynamic Optical Imaging Center, College of Chemistry and Molecular Engineering, Peking University, Beijing 100871, People's Republic of China

Email: H.L.: chemhualu@pku.edu.cn; E.Q.C.: eqchen@pku.edu.cn

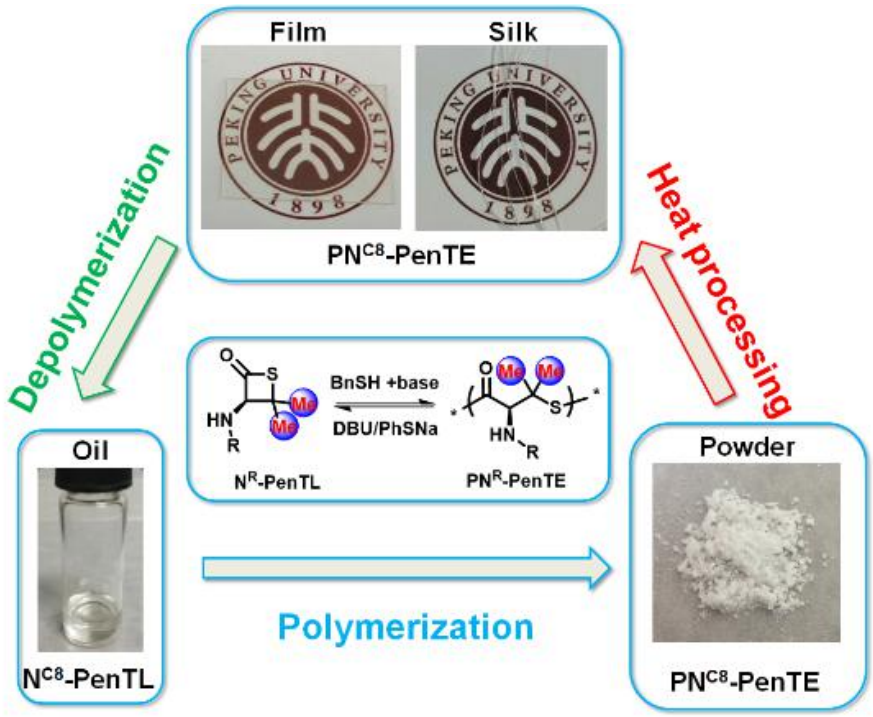

Abstract: To access infinitely recyclable plastics, one key is to design thermodynamically neutral systems based on dynamic bonds for easy manipulation of the polymerization and the reverse depolymerization under low energy cost. Here, we present the controlled ring-opening polymerization of various penicillamine-derived β-thiolactones and the highly specific depolymerization of the resultant polythioesters (PN^R-PenTE) for complete monomer recycling. The *gem*-dimethyl group confers better ROP control by reducing the activity of the chain-end thiolate groups and stabilizing the thioester linkages in the polymer backbone. High molar mass and narrow dispersity PN^R-PenTE are conveniently accessible at room temperature bearing well-defined end groups and tunable side chains. PN^R-PenTE can be tailored with water solubility, and/or be easily fabricated into persistent films or fibers with interesting thermal and mechanical properties. Most importantly, PN^R-PenTE can be recycled to pristine enantiopure β-thiolactones at >95% conversion in a well-controlled unzipping fashion within min to hours at room temperature. Overall, this work may streamline the rapid development of a wide range of polythioesters with immense application potential as self-immolative building blocks, high value biomaterials, and sacrificial domain for nanolithography.

Introduction

The annual global production of plastics has increased more than 20-fold since 1964, reaching 348 million metric tons in 2017.[1] The rapid accumulation of petroleum-based plastic wastes has created one of the greatest environmental crises in the world.[2] Single-use plastics have been banned in Europe, while other countries (e.g. China) are expected to enact similar regulations in the near future. In conjunction to developing methodologies for the degradation of existing plastics,[3-5] the need for infinitely recyclable new plastics from renewable feedstock has received vast global attention.[6-12] As previously suggested by Endo, Albertsson, and others, it is imperative to design thermodynamically near-equilibrium systems for easy manipulation of the polymerization and reverse depolymerization.[13-17] Along this direction, many biomass and CO_2 derived synthetic polymers, mainly polyesters and polycarbonates, have shown their capability of establishing a circular economy of monomer-polymer-monomer.[18-32] Despite the advancement, the development of recyclable polymers under mild condition and at low energy cost have been limited. Polymers such as poly(γ-butyrolactone) can be completely recycled, elegantly demonstrated by Chen *et al.*, but the polymerization of the non-strained γ-butyrolactone requires high energy input (-30 – -60 ^{o}C) due to unfavorable thermodynamics (ΔG_P° = + 6.4 kJ/mol). Moreover, both the polymerization and depolymerization need strong catalysts and demanding conditions owing to relative high energy barrier for ester activation.[19,31] Thus, introducing more dynamic bonds to thermodynamically near-equilibrium system could be a viable but underdeveloped

approach to design sustainable polymers.

Polythioesters (PTE) are one such intriguing example because of the dynamic thioester bonds in their backbones, which are more reactive than their oxoester analogues.[33-45] However, PTEs are significantly less explored than polyesters due to a lack of controlled ring-opening polymerization (ROP) methods that convert thiolactones to high-molar-mass (M_n) polymers with narrow dispersity ($Đ$). A few recent advances by Bowman,[35] Lu,[38] and Gutekunst[37] achieved modest-to-good control of PTEs, but the recycling of the polymers were not investigated. We have recently reported the controlled synthesis of PTEs from 4-hydroxyproline-derived thiolactone (ProTL) monomers and demonstrated that the polymers can be conveniently depolymerized.[46] Nevertheless, these polymers are found to be brittle due to their relatively rigid prolyl backbone, necessitating further optimization of appropriate side chain and new backbone design.

An interesting study by Suzuki and coworkers reported the synthesis of PTEs from a cysteine-derived β-thiolactone (CysPTE).[47] The use of amino acid as the feedstock is a smart approach to access chiral and semicrystalline polymers. Unfortunately, the resulting polymers are characterized by relatively low molar mass (typical M_n < 10 kg/mol), broad dispersity ($Đ$ ~ 1.6-2.4), and mixed linear/cyclic topologies. The underlying challenges include undesirable chain transfer, reshuffling, and backbiting, all or at least partially attributable to the extensive transthioesterification side reactions. CysPTEs are also difficult to depolymerize for monomer recycling owing to the highly strained 4-membered β-thiolactone ring. One

classical strategy of accelerating ring closure and stabilizing strained rings in physical organic chemistry is the *gem*-disubstituent effect.[48-49] We thus hypothesize that the introduction of a geminal dimethyl (*gem*-DM) group on the four-membered ring could tune the thermodynamics to near equilibrium for improved propensity of depolymerization, and in the meantime mitigate the reactivity of both the chain ends and backbone for reduced transthioesterification (Scheme 1). Notably, such monomers can be easily produced and tailored with various side chains starting from a naturally occurring amino acid, D-penicillamine.[50-51]

Scheme 1

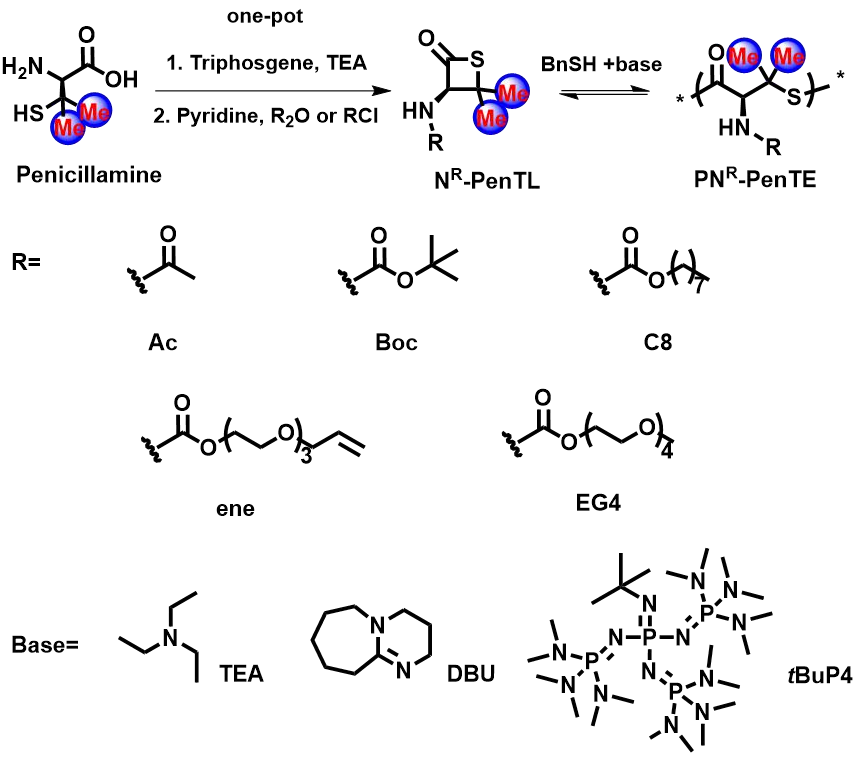

Results and Discussion

Controlled polymerization

We first synthesized five penicillamine-derived β-thiolactone monomers (N^{R}-PenTL) with different side-chains (Scheme 1B), including N^{Ac}-PenTL and N^{Boc}-PenTL as white crystals, as well as N^{C8}-PenTL, N^{ene}-PenTL, and N^{EG4}-PenTL as colorless oils (^{1}H and ^{13}C NMR, HR-MS and XRD in Figure S1-S16). Notably, the monomer synthesis is a simple and robust one-pot process and can be easily scaled up to ten-gram scale in one batch in the laboratory. The ROP of each substrate was then initiated by benzyl mercaptan and catalyzed by an organobase of suitable basicity (Scheme 1B). No ROP of N^{Ac}-PenTL or N^{Boc}-PenTL was observed (entry 1-2, Table 1), likely a result of their limited solubility (less than ~90 mg/mL in THF), which is lower than the equilibrium monomer concentration. We therefore focused our effort on the ROP of the three liquid monomers because they were substantially more soluble in common organic solvents or could be even executed for bulk polymerization. We measured the $[M]_{eq}$ of N^{ene}-PenTL at various temperatures to draw the Van't Hoff plot (Figure S17). Based on the linear regression, the enthalpy ($\Delta H_P°$) and entropy ($\Delta S_P°$) changes of the ROP were calculated to be -9.4 kJ mol^{-1} and -28.1 J mol^{-1} K^{-1}, respectively. This, in turn, gave a $\Delta G_P°$ of -1.0 kJ mol^{-1} (-0.24 kcal mol^{-1}) at 25 °C.

To increase reaction efficiency, we conducted bulk polymerization of N^{ene}-PenTL and N^{C8}-PenTL at room temperature at a feeding monomer/initiator ratio (M/I) of 100/1. To our gratification, the ROP of N^{ene}-PenTL, catalyzed by a weak organobase, triethylamine (TEA, pK_a^{DMSO} = 9.0),[52] afforded the desired polymer product

PN^{ene}-PenTE (^{1}H NMR in Figure S18) with a considerably larger M_n and narrower dispersity (entry 3, Table 1; M_n = 19.4 kg/mol, $Đ$ ~ 1.10) compared to similar PTEs synthesized previously from CysTLs (M_n ~8.8 kg/mol, $Đ$ ~ 2.4) at the same M/I ratio.[47] Replacing TEA with 0.1 equivalent of 1,8-diazabicyclo(5.4.0)undec-7-ene (DBU), a stronger base with a pK_a^{DMSO} of 12,[52] greatly accelerated the ROP reaction (entry 4-7, Table 1 and Fig. 1A) while preserving the controllability, as evidenced by the unimodal peaks in size-exclusion chromatography (SEC) analysis. Increasing the M/I ratio resulted in a corresponding linear elevation in the M_n of PN^{ene}-PenTE (Fig. 1A). The DBU-catalyzed ROP of N^{ene}-PenTL also demonstrated other typical features of controlled polymerization, such as the observation that the monomer conversion displayed a linear relationship with M_n (Fig. 1B). The ROP of N^{C8}-PenTL showed very similar controllability to that of N^{ene}-PenTL (entry 8-10, Table 1). For example, DBU-catalyzed formation of PN^{C8}-PenTE (^{1}H NMR in Figure S19) at a M/I ratio of 100/1 exhibited a M_n of 20.1 kg/mol and $Đ$ of 1.21 (entry 8, Table 1). By employing *t*BuP4, a phosphazene superbase with a pK_a^{DMSO} of 30.3,[52] the M_n could be further boosted to 52.4 and 70.6 kg/mol at a M/I ratio of 250/1 and 350/1, respectively, while maintaining a $Đ$ less than 1.30 (entry 9-10, Table 1). Copolymerization of N^{C8}-PenTL and N^{Boc}-PenTL mixture gave a random copolymer with a M_n of 14.1 kg/mol and a $Đ$ ~1.24 (entry 11, Table 1). The ROP of N^{EG4}-PenTL, a monomer containing an oligothethylene glycol side chain, afforded a PEG-like polymer PN^{EG4}-PenTE (^{1}H NMR in Figure S20) also with satisfactory control (entry 12, Table 1).

Table 1. Ring-Opening polymerization of N^{R}-PenTL [a]

entry	monomer	base	$[M]_0/[I]_0/[base]_0$	time (h)	M_n^{cal} (g mol^{-1})[b]	M_n^{obt} (g mol^{-1})[c]	$Đ$[d]	conv.[e]
1	N^{Ac}-PenTL	TEA	50/1/1	24	8700	-	-	0
2	N^{Boc}-PenTL	TEA	50/1/1	24	11600	-	-	0
3	N^{ene}-PenTL	TEA	100/1/1	72	34700	19400	1.10	61%
4	N^{ene}-PenTL	DBU	30/1/0.1	1	10400	6400	1.11	58%
5	N^{ene}-PenTL	DBU	50/1/0.1	3	17400	9900	1.09	60%
6	N^{ene}-PenTL	DBU	75/1/0.1	4.5	26000	13700	1.15	61%
7	N^{ene}-PenTL	DBU	100/1/0.1	6	34700	18500	1.14	59%
8	N^{C8}-PenTL	DBU	100/1/1	0.3	28700	20100	1.21	70%
9	N^{C8}-PenTL	*t*BuP4	250/1/1	20	71800	52400	1.26	69%
10	N^{C8}-PenTL	*t*BuP4	350/1/1	24	100500	70600	1.23	70%
11	N^{Boc}-PenTL /N^{C8}-PenTL	DBU	30/70/0.5/1	1	27000	14100	1.24	42% /56%
12	N^{EG4}-PenTL	DBU	50/1/1	6	18300	13900	1.30	57%

[a]Polymerizations were initiated with benzyl mercaptan in a glovebox at room temperature. All entry were performed as bulk polymerizations except for entry 1-2 that were conducted in THF. [b]M_n^{cal} = calculated number-average molar mass based on the feeding M/I ratio. [c]M_n^{obt} = obtained number-average molar mass determined by SEC in DMF with 0.1 M LiBr. [d]$Đ$ = dispersity. [e]Monomer conversion, determined by ^{1}H NMR.

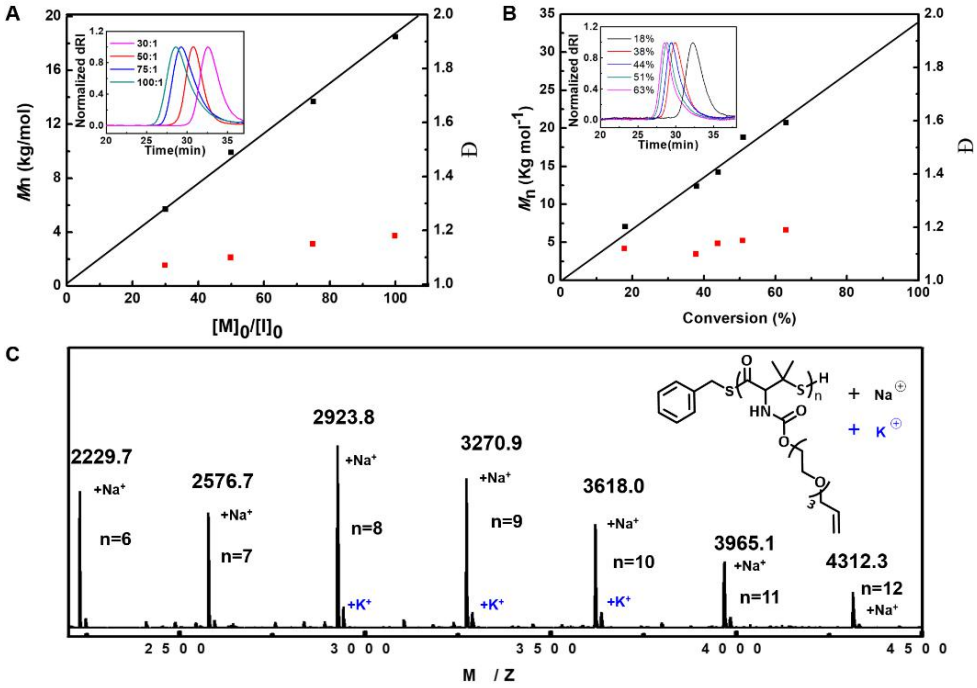

Figure 1. Bulk ROP of benzyl mercaptan-mediated and DBU-catalyzed N^{ene}-PenTL. (A) Plots of M_n and $Đ$ as a function of the $[M]_0/[I]$ ratio. Inset: Overlay of SEC curves at different $[M]_0/[I]$ ratios. (B) Plots of M_n and $Đ$ as a function of monomer conversion at the $[M]_0/[I]$ ratio of 100/1. Inset: Overlay of SEC curves at different monomer conversions. (C) MALDI-TOF mass spectrum of benzyl mercaptan-initiated PN^{ene}-$PenTE_{15}$.

Facile Functionalization

Next, we examined the chain-end group of the resulting PN^{ene}-PenTE and its ability to undergo post-polymerization modification. Matrix-assisted laser desorption ionization-time of flight (MALDI-TOF) mass spectrum of benzyl mercaptan-initiated PN^{ene}-$PenTE_{15}$ contained only one set of molecular ion peaks with a spacing of 347 Da between two adjacent peaks, which corresponded to the molar mass of the monomer (Figure 1C). Moreover, the end groups were unambiguously assigned to the initiating $PhCH_2S$– group on the α-end and free tertiary thiol on the ω-terminus (Figure 1C, plus Na^+ or K^+). When the ROP was quenched with a small molecular capping agent such as iodoacetamide, MALDI-TOF analysis gave exclusively PN^{ene}-$PenTE_{15}$ bearing $PhCH_2S$– and $–CH_2CONH_2$ as the α- and ω- end group, respectively (Figure S21). Similarly, PN^{C8}-PenTE also gave well-defined chain end groups in the MALDI-TOF analysis (Figure S22-23). Moreover, PN^{ene}-PenTE (ω-end capped) was found to withstand typical UV-triggered thiol-ene reactions and the side chain alkenes were converted to long alkyls (Figure S24) or anionic sulfate (Figure S25) groups almost quantitatively. Notably, the ω-end uncapped PN^{C8}-PenTE was stable in solution when mixing with 10 equiv benzyl mercaptan at 65 ^oC for 12 h without base or UV (Figure S26). Together, the results indicated that not only the chain ends but also the side chain groups were easily tunable, allowing facile introduction of a variety of functionalities.

Thermal and mechanical property

Next, we studied the thermal properties of PN^{C8}-PenTE (M_n ~70.6 kg/mol) via thermogravimetric analysis (TGA) and differential scanning calorimetry (DSC). PN^{C8}-PenTE showed a 5%-weight-loss decomposition temperature (T_d) of ~192 °C, regardless of the capping status at the ω end (Figure S27).

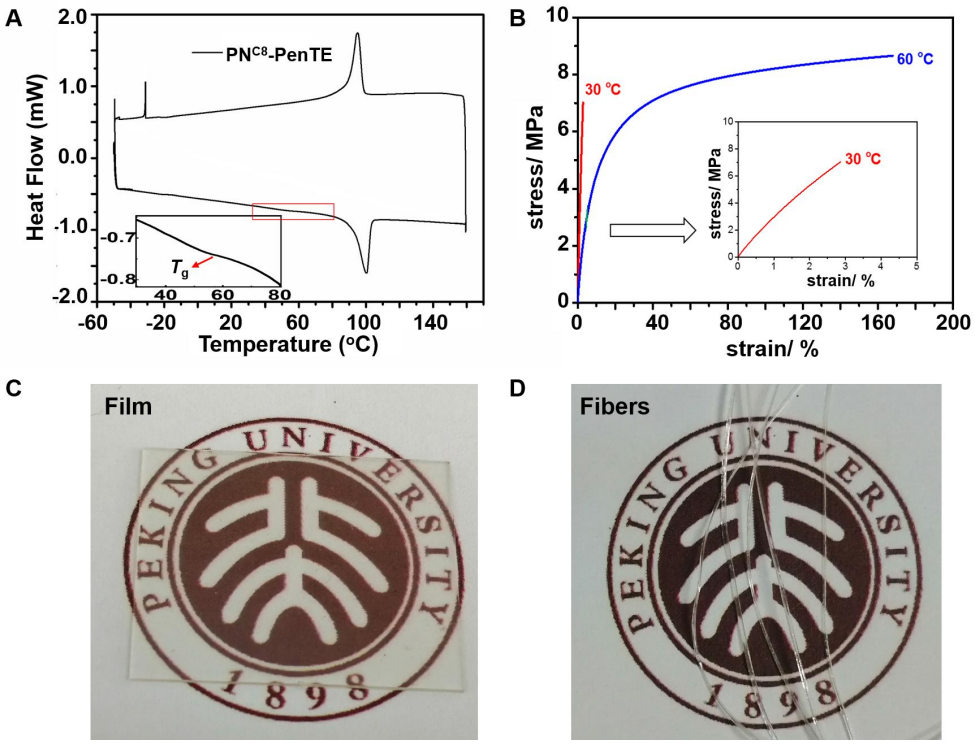

Figure 2. (A) DSC curve of PN^{C8}-PenTE. (B) Stress-strain curves of PN^{C8}-PenTE test by DMA using a constant force rate of 0.5 N/min at 30 (red) or 60 °C (blue). (C-D) The photographs of PN^{C8}-PenTE as a transparent film (C) and fibers (D) obtained by hot compression and melting drawing at 140 °C, respectively.

DSC result depicted a weak glass transition at the temperature of ~50 °C (T_g) and a large endotherm peaked at ~100 °C that corresponds to crystal melting in the heating scan (Figure 2A). Upon cooling, an exothermic peak was observed at the temperature slightly lower than the melting temperature (T_m). Dilatometry test suggested that the

T_g and T_m of the same polymer was ~ 45 and ~100 °C (Figure S28), respectively, which agreed well with the results in DSC. In the tensile test using dynamic mechanical analysis (DMA), PN^{C8}-PenTE showed a Young's modulus of 300 MPa at 30 °C and a catastrophic facture before yielding with a strain of 2.8% (Figure 2B). Above the T_g, the Young's modulus reduced to 110 MPa and on the other hand, the breaking strain increased to 170% at 60 °C (Figure 2B). PN^{C8}-PenTE can be manufactured into a transparent film by hot compression or flexible fibers by melt drawing at 140 °C with no detectable decomposition (Figure 2C-D).

Controlled and Complete Depolymerization

To investigate and optimize the depolymerization of the ω-end uncapped PN^{C8}-PenTE, we tested all reactions in diluted $CDCl_3$ (initial polymer concentration = 5.0 mg/mL) by employing various bases and temperatures. When PN^{C8}-PenTE was mixed with 0.05 equiv DBU (relative to the number of polymer chains) at 65 °C, the gradual regeneration of N^{C8}-PenTL was confirmed by ^{1}H NMR and SEC. The conversion of depolymerization exhibited an inverse linear relationship with the remaining M_n of the polymer (Figure 3B). Moreover, only unimodal peaks were observed in the SEC analysis of the depolymerization of PN^{C8}-PenTE, implying no oligomerization occurred (Figure 3C). All these data offered convincing evidence for a domino-like unzipping depolymerization process. However, $[\alpha]_D$ test of the recycled monomer indicated racemization (Table 2, entry 1 and 2). Interestingly, at reduced temperatures such as 25 °C, PN^{C8}-$PenTE_{40}$ was completely depolymerized (>95%) into enantiopure

monomers (Figure 3D and entry 3, Table 2) within 4h, catalyzed by 0.1 equiv DBU. Thus, it appeared that lower temperature could prevent racemization effectively. This notion was further confirmed by the fact that complete depolymerization without racemization of PN^{C8}-$PenTE_{40}$ was achievable within 10 min by using 1 equiv DBU at -25 °C (entry 4, Table 2). The depolymerization can also be catalyzed by 1.0 equiv sodium thiophenolate (PhSNa), a weaker base but strong nucleophile, which gave >95% conversion within 2h at ambient temperature, again with no detectable racemization (entry 5, Table 2). PN^{ene}-PenTE showed a very similar result to PN^{C8}-PenTE in depolymerization (entry 6-7, Table 2 and Figure S29). Of note, the ω-end-capped PN^{ene}-PenTE remained almost unchanged when mixed with 0.1 eq DBU at 25 °C for 12 h (Figure S30), suggesting the depolymerization can only be triggered from the ω-end, in line with the observation of Figure 3B-C.

Table 2. Depolymerization of PN^{R}-PenTE in dilute solution[a]

entry	monomer/polymer	catalyst	equiv.[b]	time (min)	temperature (°C)	$[\alpha]_D^{17.2}$[c]
1	N^{C8}-PenTL	-	-	-	-	-35.8
2	PN^{C8}-PenTE	DBU	0.05	1	65	0
3	PN^{C8}-PenTE	DBU	0.1	240	25	-34.2
4	PN^{C8}-PenTE	DBU	1	10	-25	-35.8
5	PN^{C8}-PenTE	PhSNa	1	120	25	-35.6
6	N^{ene}-PenTL	-	-	-	-	-37.4
7	PN^{ene}-PenTE	DBU	0.1	240	25	-36.6

[a]All entry were conducted in THF at a concentration of 5.0 mg/mL. [b]Relative to the number of polymer chains. [c]Specific optical rotation, determined by polarimeter in THF at 17.2 °C.

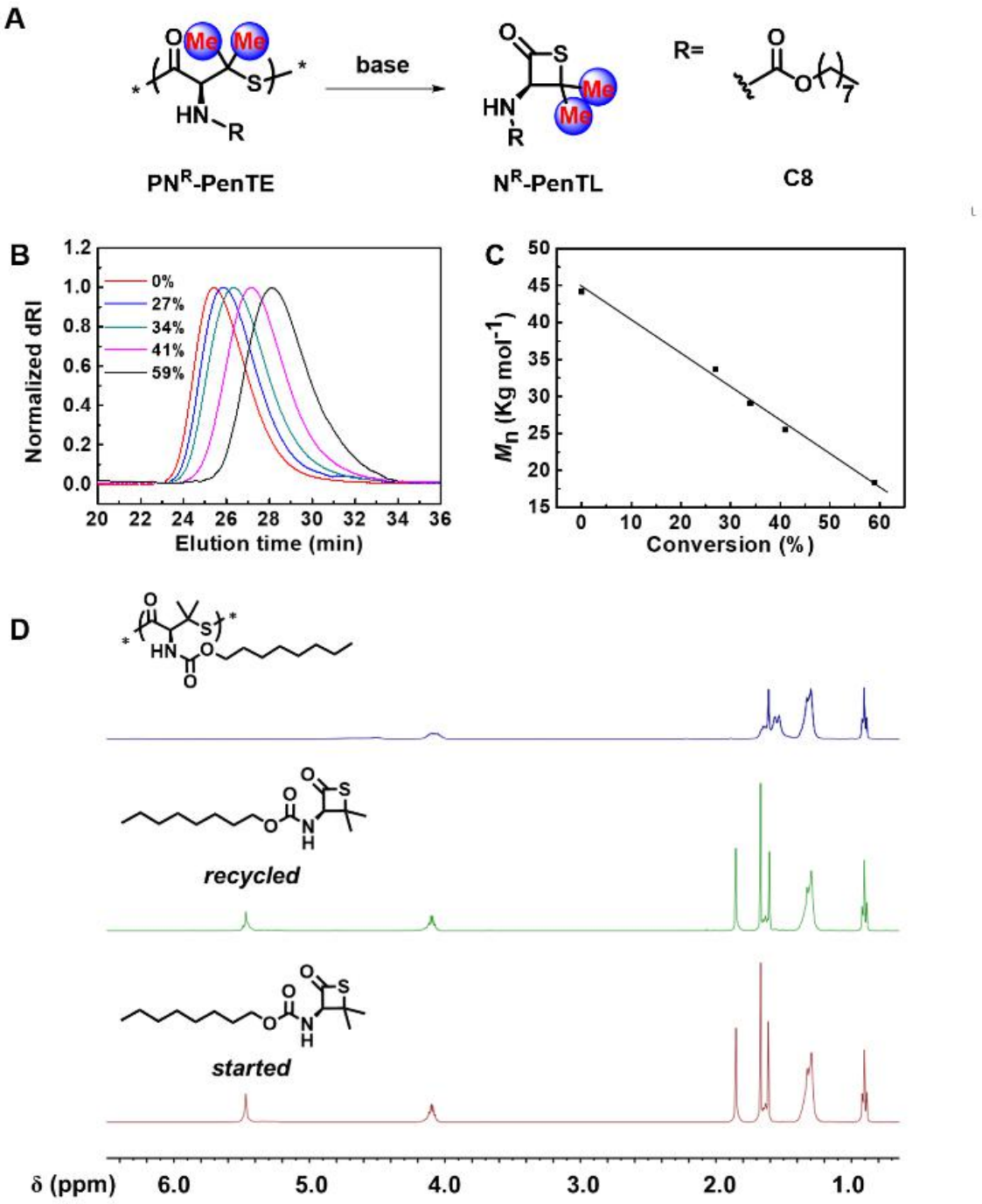

Figure 3. DBU-catalyzed depolymerization of PN^{C8}-PenTE. (A) Scheme of PN^{C8}-PenTE depolymerization. (B) Overlay of SEC curves at different depolymerization conversions. (C) Plot of the remaining M_n of PN^{C8}-PenTE as a function of the conversion of the depolymerization.(D) Overlay of the ^1H NMR spectra in $CDCl_3$ of PN^{C8}-$PenTE_{40}$ (top), recycled N^{C8}-PenTL after depolymerization (middle), and the started N^{C8}-PenTL as a reference (bottom).

Mechanism of ROP and depolymerization

We further studied the ROP and depolymerization of N^{R}-PenTL by density functional theory (DFT) calculation and molecular dynamics (MD) simulation. To simplify the calculation, N^{Ac}-PenTL was used as a model monomer and the reactive chain end was considered to consist of a dissociated anionic thiolate. The free energies of key intermediates (INT) and transition states (TS) in both the chain propagation and chain transfer were summarized in Figure 4A. The free energy change of the ROP was calculated to be 0.8 kcal/mol (INT_1 to INT_2), agreed well with the previous Van't Hoff plot (-0.24 kcal/mol). The energy barrier for the chain propagation (INT_1 to $2TS_1$) and chain transfer (INT_1 to TS_2) was 6.6 and 19.2 kcal/mol, respectively (Figure 4B). The ~12.6 kcal/mol difference in energy barrier, according to the Helmholtz equation, suggested that the rate constants of the two pathways differed from each other by an order of magnitude of ~6, which ensured that the ROP would proceed in a highly controlled fashion as we observed. Interestingly, the energy barrier of chain propagation and chain transfer in the ROP of N^{Ac}-CysTE were substantially lower, 0.5 and 2.2 kcal/mol, respectively (Figure S31). Such low energy barriers suggested that the rate of both propagation and transfer reactions were fast and it was difficult to minimize chain transfer.

For depolymerization of PN^{Ac}-PenTE, the energy barrier was 5.8 kcal/mol (INT_2 to TS_1, Figure 4B), which served as a key contributor to the amenability of PN^{R}-PenTE to depolymerization. On the other hand for N^{Ac}-CysTE, the free energy change was so favored for the ROP (–14.4 kcal/mol), making the reverse

depolymerization pathway highly unfavorable thermodynamically (C-INT_2 to C-TS_1, Figure S31). DFT calculation further suggested that in the low energy conformation of PN^R-PenTE, the terminal tertiary thiolate and the adjacent thioester took a gauche conformation with a *S---C=O* distance of ~2.96 Å and a *S-C-C-CO* dihedral angle (Ψ) of 66.4º (Figure 4C), which required no extra rotary energy for the ring-closing depolymerization. On the contrary, the low energy conformation of N^{Ac}-CysTE was the staggered conformation in which the same *S---C=O* distance was ~4.17 Å (Figure 4C). All atom MD simulation (Figure 4D-E) of the 20-mer of PN^{Me}-PenTE also suggested that the most populated conformation (Ψ=67.7%) is characterized by an average *S---C=O* distance of 3.4 Å between the terminal thiol and its adjacent thioester carbon, whereas the staggered conformations with a longer distance (4.20 Å in average) were less populated (18.2%). This restrained conformation is a clear indication of the Thorpe–Ingold effect induced by the *gem*-DM.[48-49]

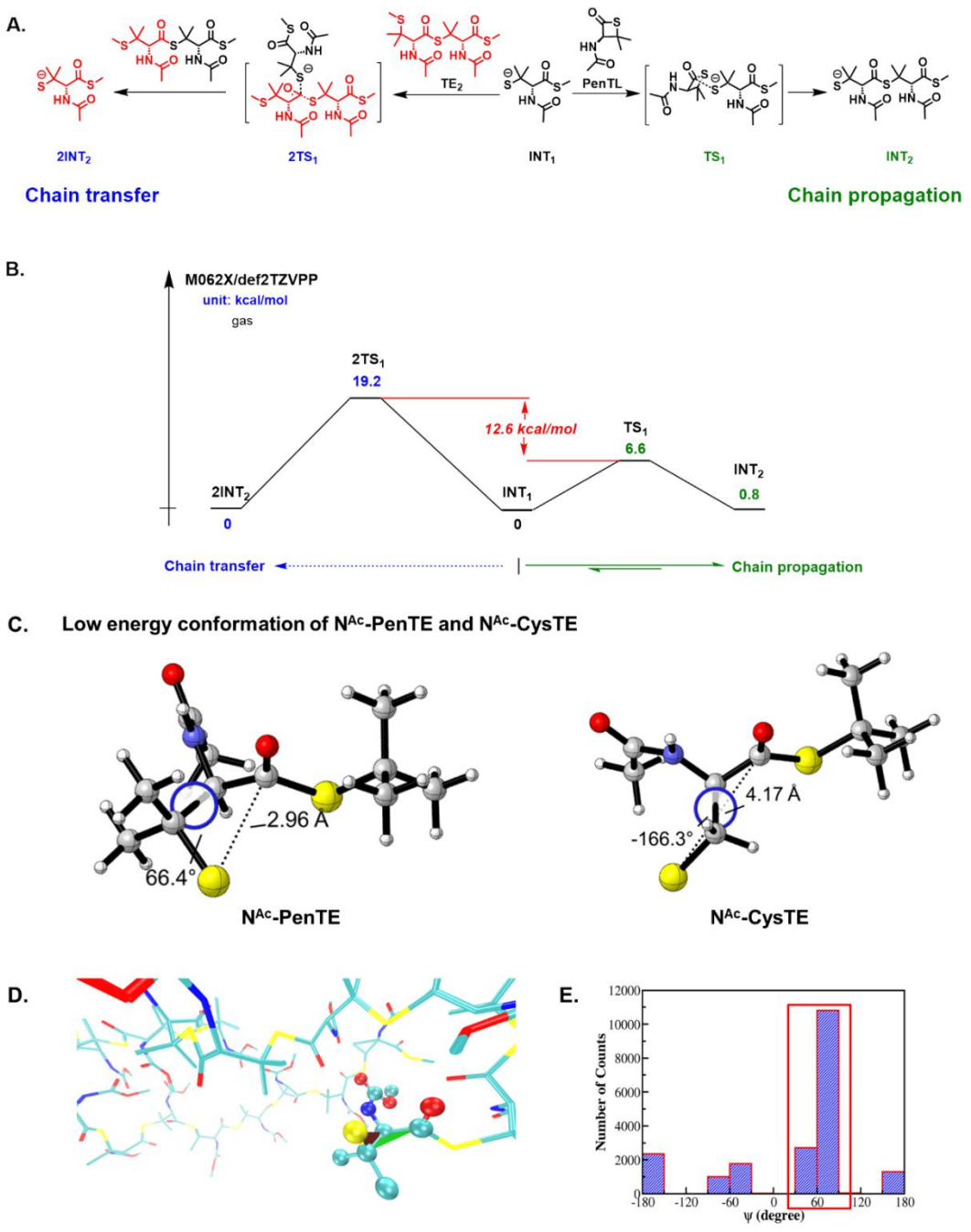

Figure 4. Mechanistic investigation of the ROP and chain transfer by DFT calculation and MD simulation. (A) Proposed chain propagation and transfer intermediates (INT) and transition states (TS) in the ROP of N^{R}-PenTL in gas. (B) Calculated free energy of each INT and TS. (C) Low energy conformation of N^{A}-PenTE and N^{Ac}-CysTE. (D) The most popular conformation of PN^{Me}-$PenTE_{20}$. (E) Ψ dihedral angle distribution of different conformations of PN^{Me}-$PenTE_{20}$.

Discussion and Conclusions

The unique thermomechanical, optical and dynamic properties of PTE polymers, coupled with a global emphasis on environmental sustainability, have propelled a resurgence in their popularity. [33,53-54] Although chemical production[45] and biosynthesis[55] of PTEs were first reported in 1968 and 2001, respectively, controlled chemical synthesis of high M_n PTEs remains a technological bottleneck due to the dynamic nature of thioesters. In this work, we achieved the first controlled ROP of β-thiolactones by introducing a *gem*-DM group on the four-membered ring (Table 1 and Figure 1). The facile access to high M_n PTEs under mild conditions could provide a significant boost to their industrial and biomedical application.

Functionalization of both the termini and side groups in PN^{R}-PenTE opens up opportunities to create novel, high-performance materials by introducing different combinations of substituents to the polymer chain. As demonstrated earlier, the *N*-octanoyloxy groups in PN^{C8}-PenTL confer semicrystallinity, increase processability and durability (Figure 2). On the other hand, PN^{EG4}-PenTE (entry 12, Table 1) exhibits excellent water solubility and degradability, making it an attractive alternative to PEG and a promising high-value biomaterial for temperature-induced self-assembly and/or therapeutic protein conjugation.[56-57] The physicochemical properties of PN^{R}-PenTE could be further expanded or fine-tuned by copolymerizing several types of monomers with different side chains (entry 11, Table 1).

Previously reported strategies for polymer recycling predominantly involved reverting back to cyclic monomers bearing a five- or six-membered ring, which are

relatively unstrained.[17,19,22,31,58] We recently succeeded in extending the scope of such regenerative building blocks to bridged bicyclic thiolactones.[46] In the current study, we further demonstrated, based on both experimental data and theoretical calculations, that the presence of *gem*-DM played a key role in enabling fast, selective and highly controlled depolymerization of PN^R-PenTEs (Figure 3 and 4). Of note, while depolymerizable polymers were not uncommon, the domino-like unzipping fashion in the depolymerization of PN^R-PenTEs (Figure 3A-B) was relatively rare. This control was again likely empowered by the presence of *gem*-DM (Figure 4C-E). It is also worth pointing out that similar ring-closure reactions that are driven by the Thorpe–Ingold effect have been frequently employed.[59-61] Thus, we envisage that our current strategy can be broadly applied to the design of various recyclable polymers beyond PN^R-PenTEs.

It should be noted that the relatively high price of penicillamine could pose a challenge to our method when applied on an industrial scale. Nevertheless, cost mitigation could potentially be achieved by further optimizing the chemical and/or biosynthetic-based routes to produce similar substrate monomer in a more affordable manner.[62] Overall, the strategy can be utilized to rapidly and efficiently generate a wide range of high-value, recyclable polymers with immense application potential as self-immolative materials,[63-64] covalent adaptable networks,[65] sacrificial domain for nanolithography, and responsive biomaterials.[53]

Supporting Information

Experimental details, ^1H and ^{13}C NMR spectra, MALDI-TOF mass spectra, SEC traces, TGA and DSC traces (PDF); X-ray crystallographic data (CIF)

Conflict of interest

The authors declare no competing financial interest.

Acknowledgements

This work is supported by the National Natural Science Foundation of China (21722401 for H.L. and 21634001 for E.Q.C.). The computation was supported by High-performance Computing Platform of Peking University. We thank Prof. Suwei Dong and Prof. Zichen Li for inspiring discussions.

Keywords: polythioester • ring-opening polymerization • monomer recycling • sustainable • near-equilibrium

References

1. Tang, X., and Chen, E.Y.X. (2019). Toward Infinitely Recyclable Plastics Derived from Renewable Cyclic Esters. Chem *5*, 284-312.

2. Geyer, R., Jambeck, J.R., and Law, K.L. (2017). Production, Use, and Fate of All Plastics Ever Made. Sci Adv *3*.

3. Jehanno, C., Flores, I., Dove, A.P., Muller, A.J., Ruiperez, F., and Sardon, H. (2018). Organocatalysed Depolymerisation of Pet in a Fully Sustainable Cycle Using Thermally Stable Protic Ionic Salt. Green Chem *20*, 1205-1212.

4. Jia, X.Q., Qin, C., Friedberger, T., Guan, Z.B., and Huang, Z. (2016). Efficient and Selective Degradation of Polyethylenes into Liquid Fuels and Waxes under Mild Conditions. Sci Adv *2*.

5. Jehanno, C., Perez-Madrigal, M.M., Demarteau, J., Sardon, H., and Dove, A.P. (2019). Organocatalysis for Depolymerisation. Polymer Chemistry *10*, 172-186.

6. Zhu, Y.Q., Romain, C., and Williams, C.K. (2016). Sustainable Polymers from Renewable Resources. Nature *540*, 354-362.

7. Albertsson, A.C., and Hakkarainen, M. (2017). Designed to Degrade Suitably Designed Degradable Polymers Can Play a Role in Reducing Plastic Waste. Science *358*, 872-873.

8. Garcia, J.M., and Robertson, M.L. (2017). The Future of Plastics Recycling Chemical Advances Are Increasing the Proportion of Polymer Waste That Can Be Recycled. Science *358*, 870-872.

9. Hillmyer, M.A. (2017). The Promise of Plastics from Plants Plant-Derived Feedstocks Are Increasingly Competitive in Plastics Production. Science *358*, 868-870.

10. Garcia, J.M., Jones, G.O., Virwani, K., McCloskey, B.D., Boday, D.J., ter Huurne, G.M., Horn, H.W., Coady, D.J., Bintaleb, A.M., Alabdulrahman, A.M.S.*, et al.* (2014). Recyclable, Strong Thermosets and Organogels Via Paraformaldehyde Condensation with Diamines. Science *344*, 732-735.

11. Zhang, X.Y., Fevre, M., Jones, G.O., and Waymouth, R.M. (2018). Catalysis as an Enabling Science for Sustainable Polymers. Chem. Rev. *118*, 839-885.

12. Tretbar, C.A., Neal, J.A., and Guan, Z.B. (2019). Direct Silyl Ether Metathesis for Vitrimers with Exceptional Thermal Stability. J. Am. Chem. Soc. *141*, 16595-16599.

13. Hocker, H., and Keul, H. (1994). Ring-Opening Polymerization and Ring-Closing Depolymerization. Adv. Mater. *6*, 21-36.

14. Endo, T., Kakimoto, K., Ochiai, B., and Nagai, D. (2005). Synthesis and Chemical Recycling of a Polycarbonate Obtained by Anionic Ring-Opening Polymerization of a Bifunctional Cyclic Carbonate.

Macromolecules *38*, 8177-8182.
15. Endo, T., and Nagai, D. (2005). A Novel Construction of Ring-Opening Polymerization and Chemical Recycling System. Macromol. Symp. *226*, 79-86.
16. Olsen, P., Odelius, K., and Albertsson, A.C. (2016). Thermodynamic Presynthetic Considerations for Ring-Opening Polymerization. Biomacromolecules *17*, 699-709.
17. Olsen, P., Undin, J., Odelius, K., Keul, H., and Albertsson, A.C. (2016). Switching from Controlled Ring-Opening Polymerization (Crop) to Controlled Ring-Closing Depolymerization (Crcdp) by Adjusting the Reaction Parameters That Determine the Ceiling Temperature. Biomacromolecules *17*, 3995-4002.
18. Sangroniz, A., Zhu, J.-B., Tang, X., Etxeberria, A., Chen, E.Y.X., and Sardon, H. (2019). Packaging Materials with Desired Mechanical and Barrier Properties and Full Chemical Recyclability. Nat. Commun. *10*, 3559.
19. Hong, M., and Chen, E.Y.X. (2016). Completely Recyclable Biopolymers with Linear and Cyclic Topologies Via Ring-Opening Polymerization of Gamma-Butyrolactone. Nat. Chem. *8*, 42-49.
20. Zhu, J.B., Watson, E.M., Tang, J., and Chen, E.Y.X. (2018). A Synthetic Polymer System with Repeatable Chemical Recyclability. Science *360*, 398-403.
21. Xu, S., Lamm, M.E., Rahman, M.A., Zhang, X., Zhu, T., Zhao, Z., and Tang, C. (2018). Renewable Atom-Efficient Polyesters and Thermosetting Resins Derived from High Oleic Soybean Oil. Green Chem. *20*, 1106-1113.
22. Liu, Y., Zhou, H., Guo, J.Z., Ren, W.M., and Lu, X.B. (2017). Completely Recyclable Monomers and Polycarbonate: Approach to Sustainable Polymers. Angew. Chem., Int. Ed. *56*, 4862-4866.
23. Liu, Y., and Mecking, S. (2019). A Synthetic Polyester from Plant Oil Feedstock by Functionalizing Polymerization. Angew. Chem., Int. Ed. *58*, 3346-3350.
24. Myers, D., Witt, T., Cyriac, A., Bown, M., Mecking, S., and Williams, C.K. (2017). Ring Opening Polymerization of Macrolactones: High Conversions and Activities Using an Yttrium Catalyst. Polymer Chemistry *8*, 5780-5785.
25. Song, Y., Ji, X., Dong, M., Li, R., Lin, Y.N., Wang, H., and Wooley, K.L. (2018). Advancing the Development of Highly-Functionalizable Glucose-Based Polycarbonates by Tuning of the Glass Transition Temperature. J. Am. Chem. Soc. *140*, 16053-16057.
26. Miyaji, H., Satoh, K., and Kamigaito, M. (2016). Bio-Based Polyketones by Selective Ring-Opening Radical Polymerization of Alpha-Pinene-Derived Pinocarvone. Angew. Chem., Int. Ed. *55*, 1372-1376.
27. Bhaumik, A., Peterson, G.I., Kang, C., and Choi, T.L. (2019). Controlled Living Cascade Polymerization to Make Fully Degradable Sugar-Based Polymers from D-Glucose and D-Galactose. J. Am. Chem. Soc. *141*, 12207-12211.
28. Saxon, D.J., Nasiri, M., Mandal, M., Maduskar, S., Dauenhauer, P.J., Cramer, C.J., LaPointe, A.M., and Reineke, T.M. (2019). Architectural Control of Isosorbide-Based Polyethers Via Ring-Opening Polymerization. J. Am. Chem. Soc. *141*, 5107-5111.
29. De Hoe, G.X., Zumstein, M.T., Tiegs, B.J., Brutman, J.P., McNeill, K., Sander, M., Coates, G.W., and Hillmyer, M.A. (2018). Sustainable Polyester Elastomers from Lactones: Synthesis, Properties, and Enzymatic Hydrolyzability. J. Am. Chem. Soc. *140*, 963-973.
30. Chen, X., Chen, G., Tao, Y., Wang, Y., Lu, X.-B., Zhang, L., Zhu, J., Zhang, J., and Wang, X. (2019). Progress in Eco-Polymers. Acta Polym. Sin. *50*, 1068-1082.
31. Zhao, N., Ren, C., Li, H., Li, Y., Liu, S., and Li, Z. (2017). Selective Ring-Opening Polymerization of Non-Strained Gamma-Butyrolactone Catalyzed by a Cyclic Trimeric Phosphazene Base. Angew. Chem., Int. Ed. *56*, 12987-12990.

32. Feist, J.D., and Xia, Y. (2020). Enol Ethers Are Effective Monomers for Ring-Opening Metathesis Polymerization: Synthesis of Degradable and Depolymerizable Poly(2,3-Dihydrofuran). J. Am. Chem. Soc. *142*, 1186-1189.

33. Aksakal, S., Aksakal, R., and Becer, C.R. (2018). Thioester Functional Polymers. Polym. Chem. *9*, 4507-4516.

34. Wang, C., Mavila, S., Worrell, B.T., Xi, W.X., Goldman, T.M., and Bowman, C.N. (2018). Productive Exchange of Thiols and Thioesters to Form Dynamic Polythioester-Based Polymers. ACS Macro Lett. *7*, 1312-1316.

35. Mavila, S., Worrell, B.T., Culver, H.R., Goldman, T.M., Wang, C., Lim, C.H., Domaille, D.W., Pattanayak, S., McBride, M.K., Musgrave, C.B.*, et al.* (2018). Dynamic and Responsive DNA-Like Polymers. J. Am. Chem. Soc. *140*, 13594-13598.

36. Espeel, P., Carrette, L.L.G., Bury, K., Capenberghs, S., Martins, J.C., Du Prez, F.E., and Madder, A. (2013). Multifunctionalized Sequence-Defined Oligomers from a Single Building Block. Angew. Chem., Int. Ed. *52*, 13261-13264.

37. Smith, R.A., Fu, G., McAteer, O., Xu, M., and Gutekunst, W.R. (2019). Radical Approach to Thioester-Containing Polymers. J. Am. Chem. Soc. *141*, 1446-1451.

38. Yue, T.J., Zhang, M.C., Gu, G.G., Wang, L.Y., Ren, W.M., and Lu, X.B. (2019). Precise Synthesis of Poly(Thioester)S with Diverse Structures by Copolymerization of Cyclic Thioanhydrides and Episulfides Mediated by Organic Ammonium Salts. Angew. Chem., Int. Ed. *58*, 618-623.

39. Bannin, T.J., and Kiesewetter, M.K. (2015). Poly(Thioester) by Organocatalytic Ring-Opening Polymerization. Macromolecules *48*, 5481-5486.

40. Ura, Y., Al-Sayah, M., Montenegro, J., Beierle, J.M., Leman, L.J., and Ghadiri, M.R. (2009). Dynamic Polythioesters Via Ring-Opening Polymerization of 1,4-Thiazine-2,5-Diones. Org Biomol Chem *7*, 2878-2884.

41. Kricheldorf, H.R., and Schwarz, G. (2007). Poly(Thioester)S. J Macromol Sci A *44*, 625-649.

42. Ghobril, C., Charoen, K., Rodriguez, E.K., Nazarian, A., and Grinstaff, M.W. (2013). A Dendritic Thioester Hydrogel Based on Thiol-Thioester Exchange as a Dissolvable Sealant System for Wound Closure. Angew. Chem., Int. Ed. *52*, 14070-14074.

43. Lutke-Eversloh, T., Fischer, A., Remminghorst, U., Kawada, J., Marchessault, R.H., Bogershausen, A., Kalwei, M., Eckert, H., Reichelt, R., Liu, S.J.*, et al.* (2002). Biosynthesis of Novel Thermoplastic Polythioesters by Engineered Escherichia Coli. Nat. Mater. *1*, 236-240.

44. Kato, M., Toshima, K., and Matsumura, S. (2007). Enzymatic Synthesis of Polythioester by the Ring-Opening Polymerization of Cyclic Thioester. Biomacromolecules *8*, 3590-3596.

45. Overberg, C.G., and Weise, J.K. (1968). Anionic Ring-Opening Polymerization of Thiolactones. J. Am. Chem. Soc. *90*, 3533-3537.

46. Yuan, J., Xiong, W., Zhou, X., Zhang, Y., Shi, D., Li, Z., and Lu, H. (2019). 4-Hydroxyproline-Derived Sustainable Polythioesters: Controlled Ring-Opening Polymerization, Complete Recyclability, and Facile Functionalization. J. Am. Chem. Soc. *141*, 4928-4935.

47. Suzuki, M., Makimura, K., and Matsuoka, S. (2016). Thiol-Mediated Controlled Ring-Opening Polymerization of Cysteine-Derived Beta-Thiolactone and Unique Features of Product Polythioester. Biomacromolecules *17*, 1135-1141.

48. Jung, M.E., and Piizzi, G. (2005). Gem-Disubstituent Effect: Theoretical Basis and Synthetic Applications. Chem. Rev. *105*, 1735-1766.

49. Bachrach, S.M. (2008). The Gem-Dimethyl Effect Revisited. J. Org. Chem. *73*, 2466-2468.

50. Chen, H., Xiao, Y.X., Yuan, N., Weng, J.P., Gao, P.C., Breindel, L., Shekhtman, A., and Zhang, Q. (2018). Coupling of Sterically Demanding Peptides by Beta-Thiolactone-Mediated Native Chemical Ligation. Chem Sci *9*, 1982-1988.

51. Wang, Y., Han, L., Yuan, N., Wang, H., Li, H., Liu, J., Chen, H., Zhang, Q., and Dong, S. (2018). Traceless Beta-Mercaptan-Assisted Activation of Valinyl Benzimidazolinones in Peptide Ligations. Chem Sci *9*, 1940-1946.

52. Tshepelevitsh, S., K?tt, A., Lokov, M., Kaljurand, I., Saame, J., Heering, A., Plieger, P.G., Vianello, R., and Leito, I. (2019). On the Basicity of Organic Bases in Different Media. Eur. J. Org. Chem. *2019*, 6735-6748.

53. Brown, T.E., Carberry, B.J., Worrell, B.T., Dudaryeva, O.Y., McBride, M.K., Bowman, C.N., and Anseth, K.S. (2018). Photopolymerized Dynamic Hydrogels with Tunable Viscoelastic Properties through Thioester Exchange. Biomaterials *178*, 496-503.

54. Mutlu, H., Ceper, E.B., Li, X., Yang, J., Dong, W., Ozmen, M.M., and Theato, P. (2019). Sulfur Chemistry in Polymer and Materials Science. Macromol. Rapid Commun. *40*, e1800650.

55. Lutke-Eversloh, T., Bergander, K., Luftmann, H., and Steinbuchel, A. (2001). Identification of a New Class of Biopolymer: Bacterial Synthesis of a Sulfur-Containing Polymer with Thioester Linkages. Microbiol-Uk *147*, 11-19.

56. Lu, J., Wang, H., Tian, Z., Hou, Y., and Lu, H. (2020). Cryopolymerization of 1,2-Dithiolanes for the Facile and Reversible Grafting-from Synthesis of Protein–Polydisulfide Conjugates. J. Am. Chem. Soc. *142*, 1217-1221.

57. Hou, Y., and Lu, H. (2019). Protein Pepylation: A New Paradigm of Protein–Polymer Conjugation. Bioconjugate Chem *30*, 1604-1616.

58. MacDonald, J.P., and Shaver, M.P. (2016). An Aromatic/Aliphatic Polyester Prepared Via Ring-Opening Polymerisation and Its Remarkably Selective and Cyclable Depolymerisation to Monomer. Polym. Chem. *7*, 553-559.

59. Huang, H.C., Wang, W.Q., Zhou, Z.F., Sun, B.H., An, M.R., Haeffner, F., and Niu, J. (2019). Radical Ring-Closing/Ring-Opening Cascade Polymerization. J. Am. Chem. Soc. *141*, 12493-12497.

60. Gutekunst, W.R., and Hawker, C.J. (2015). A General Approach to Sequence-Controlled Polymers Using Macrocyclic Ring Opening Metathesis Polymerization. J. Am. Chem. Soc. *137*, 8038-8041.

61. Lee, H.K., Lee, J., Kockelmann, J., Herrmann, T., Sarif, M., and Choi, T.L. (2018). Superior Cascade Ring-Opening/Ring-Closing Metathesis Polymerization and Multiple Olefin Metathesis Polymerization: Enhancing the Driving Force for Successful Polymerization of Challenging Monomers. J. Am. Chem. Soc. *140*, 10536-10545.

62. Kulkarni, G.M., Kulkarni, S., and Sharma, N. (2018). A novel, feasible and cost effective process for the manufacture of D–penicillamine. Patent WO 2018/134836 A1, filed August 21, 2017, and published July 26, 2018.

63. Sagi, A., Weinstain, R., Karton, N., and Shabat, D. (2008). Self-Immolative Polymers. J. Am. Chem. Soc. *130*, 5434-5345.

64. Peterson, G.I., Larsen, M.B., and Boydston, A.J. (2012). Controlled Depolymerization: Stimuli-Responsive Self-Immolative Polymers. Macromolecules *45*, 7317-7328.

65. Bowman, C.N., and Kloxin, C.J. (2012). Covalent Adaptable Networks: Reversible Bond Structures Incorporated in Polymer Networks. Angew. Chem., Int. Ed. *51*, 4272-4274.